Transonic inviscid flows past thin airfoils : A new numerical method and global stability analysis using MatLab

Rui M. S. Pereira and Jitesh S. B. Gajjar

***Abstract*—In this paper we discuss a novel accurate method for computing transonic flow over lifting and non-lifting aerofoils as governed by the steady Kárman-Guderlay equation. The method is based on using finite-differences in the streamwise direction combined with spectral collocation in the other direction. This is combined with Newton iteration and a direct method for the resulting linear system. The method is fast and very robust and we are able to compute steady flows with strong shocks. Some examples considering both the symmetric and the non symmetric cases are shown and grid size study is also presented. The work has been extended to discuss the stability of the computed flows using methods based on a global stability analysis. This leads to a generalized eigenvalue problem and some results are presented. One advantage of the current approach is that for small grid sizes it is possible do the analysis using MATLAB.**

***Index Terms*—Transonic flows, Kárman Guderley, Chebyshev collocation points, stability, generalised eigenvalue problem.**

I. INTRODUCTION

The study of transonic flows is motivated in part by the observation that many modern airplane carriers operate most efficiently when cruising at speeds which fall in the transonic range, that is close to the speed of sound. Mathematically the study of transonic flows is fascinating because the governing equations are nonlinear and of mixed type. A review of the history and mathematical development of the subject can be found in the book by [1] and the development of computational methods for the solution of transonic flow problems is surveyed in [2], [3] and [4].

Aerodynamic flutter is a phenomenon whereby small perturbations in the flow can magnify and cause vibrations of the aircraft wing and airframe. In many instances these can persist as self-excited oscillations and can be destructive. It has been known for some time that flutter is more pronounced when aircraft are operating in the transonic regime. The study of aerodynamic flutter is a complex subject in its own right and for transonic aerodynamics the coupled fluid flow and structure interaction poses significant difficulties for the computational scientist, see for example the review by [5]. For this reason the bulk of the work to date in this area has involved the study of the decoupled problem, or with simplified fluid dynamics. In [6] for instance, a thin plate model is used for the aeroelasticity and the transonic small disturbance equation is used for the aerodynamics. By taking deviations about a zero basic state, a complicated nonlinear integro-differential evolution equation is derived for the disturbances. The mathematical aspects of the flutter phenomenon and the intrinsic complexities are explained clearly in the review article by [7].

R. Pereira is with the Department of Mathematics and Applications, University of Minho, Azurem, 4810 Guimaraes, Portugal. e-mail: rmp@mct.uminho.pt

J. S. B. Gajjar is with the School of Mathematics, University of Manchester, Manchester M13 9PL, UK. e-mail j.gajjar@manchester.ac.uk

The main aims of the current work are to develop tools for studying the development of instabilities in unsteady transonic flows. Arguably, instabilities in transonic flows are intimately connected with flutter and an understanding of the main instability mechanisms can aid in our understanding and developing models for predicting flutter. In recent work at the University of Manchester methods to compute global instability modes in a number of highly non-parallel flows have been developed. With the global instability approach disturbances to an underlying base flow are assumed to be proportional to $e^{\lambda t}$, and the governing linearized equations lead to a *partial differential eigenvalue problem* for determining the eigenvalues λ and eigenfunctions which depend on the spatial variables. The approach is quite distinct from the usual normal mode approach combined with a parallel flow approximation. The flows that we are interested in studying are highly non-parallel and such crude approximations are not applicable. These techniques have been used successfully to study instabilities in a number of different flow configurations such as the two-dimensional flow in a lid-driven cavity [8], subsonic flow past corners [9].

The purpose of this paper is to to show how these ideas can be extended to first compute steady flows past lifting and non-lifting aerofoils as governed by the Kárman-Guderlay equation and then examine their instability using the global stability approach.

The numerical method we have used is a novel technique in which we combine finite differences in one direction with spectral collocation in the other direction. For transonic flows the different types of computational stars are handled according to the type of point we have (subsonic, supersonic, sonic or shock point). This is described in detail in the papers by [10] and later by [11], and in in the book [1]. The method is particularly efficient for the steady case and allows one to study the generalized eigenvalue problem which arises from the global stability analysis.

Below in sections 2 and 3 we discuss the governing equations and numerical techniques used. In sections 4 and 5 we present results for symmetric aerofoils (non lifting case) and non-symmetric aerofoils (lifting case). Some results of the stability analysis are given in section 6 and some suggestions on future work are also given.

II. The flow in the Inviscid part of the domain

The governing equation may be obtained using asymptotic methods as described in [1].

The starting point is the full potential equation:

$$(a^2 - U^2)\Phi_{xx} - 2UV\Phi_{xy} + (a^2 - V^2)\Phi_{yy} = 0, \quad (1)$$

$$\frac{1}{2}(\Phi_x^2 + \Phi_y^2) + \frac{a^2}{\gamma - 1} = \frac{U_\infty}{2} + \frac{a_\infty^2}{\gamma - 1}, \quad (2)$$

where Φ represents the velocity potential, a is the local speed of sound, U_∞ is the velocity in the far field, a_∞ is the speed of sound in the far field, and $M_\infty = U_\infty/a_\infty$ is the free-stream Mach number. The velocity components (U, V) are defined as follows,

$$U = \Phi_x, \quad V = \Phi_y.$$

The density ρ and pressure p can be determined via the relationships,

$$\rho^{\gamma-1} = M_\infty^2 a^2; \quad p = \frac{\rho^\gamma}{\gamma M_\infty^2},$$

where γ is the ratio of specific heats.

In order to define the boundary conditions we assume that the flow is uniform in the far field and that the flow is tangent to the airfoil on its surface. To construct this theory we also assume that we have a thin aerofoil with width ($\delta \to 0$) and that the air flow speed is close to sonic so $M_\infty^2 = 1 - k\mu(\delta), \quad \mu(\delta) \to 0$ where k is the transonic similarity parameter and μ is a function of the airfoil width (δ). The oncoming flow is assumed to be aligned with the x-direction.

Let the airfoil be defined by,

$$y = \delta F(x),$$

then we can write the impermeability condition as,

$$\Phi_y(x, \delta F(x)) = \delta F'(x) U(x, \delta F(x)).$$

If we use non dimensional variables,

$$U = uU_\infty, V = vU_\infty,$$

then the full potential equation (1) becomes,

$$(\frac{a^2}{U_\infty^2} - u^2)\Phi_{xx} - 2uv\Phi_{xy} + (\frac{a^2}{U_\infty^2} - v^2)\Phi_{yy} = 0.$$

The expansion for Φ is described in [Cole and Cook, 1986] [1] and is given by,

$$\Phi(x, y, M_\infty, \delta) = U_\infty(x + \epsilon(\delta)\phi(x, y, k) + ...).$$

It is well known that as $M_\infty \to 1$, the perturbations extend in the y direction significantly. Because of this, we will use the stretched coordinate,

$$Y = \beta(\delta) y(\delta).$$

If we also write the second equation (2) in a non dimensional form, use Taylor expansions for the components of these rewritten equations, and finally consider only the leading order terms, we obtain via the principle of the least degeneration,

$$\beta = \delta^{\frac{1}{3}}, \quad \mu = \epsilon = \delta^{\frac{2}{3}}. \quad (3)$$

Taking (3) into account the governing equations and boundary conditions reduce to

$$\phi_{xx}(k - \phi_x(\gamma + 1)) + \phi_{YY} = 0, \quad (4)$$

$$\phi_x = \phi_Y = 0, \quad x^2 + Y^2 \to \infty, \quad (5)$$

$$\phi_Y(Y = 0) = F'(x), \quad (6)$$

where (4) is the so called Kárman-Guderley equation. We can calculate the pressure field using,

$$\frac{p}{p_\infty} = 1 - \delta^{\frac{2}{3}}\phi_x + ...$$

Next we write (4) in conservative form as follows,

$$\frac{\partial}{\partial x}(k\phi_x - \frac{\gamma + 1}{2}\phi_x^2) + \phi_{YY} = 0, \quad (7)$$

and, if we denote,

$$\psi = kx - (\gamma + 1)\phi \quad (8)$$

then, we may rewrite (7) as,

$$(\frac{\psi_x^2}{2})_x + \psi_{YY} = 0. \quad (9)$$

The boundary conditions become,

$$\psi(x^2 + Y^2 \to \infty) = 0, \quad \psi_Y(Y = 0) = -(\gamma + 1)F'(x). \quad (10)$$

In the next section we discuss the numerical method used to solve the problem described above.

III. The numerical method

In order to solve the problem (9)-(10), we used finite differences for the derivatives in the x direction and a Chebyshev collocation method to describe the derivatives in the Y direction. As described in [1] each point of the domain may be either subsonic, sonic, supersonic or a shock point. The way to deal with each point is different as we will see later. Let,

$$P = (\frac{\psi_x^2}{2}),$$

then equation (9) becomes,

$$P_x + \psi_{YY} = 0. \quad (11)$$

Let $(\psi_x)_{i+1/2,j}$ represent the derivative with respect to x of ψ at the point $(x_{i+1/2}, Y_j)$ (see Fig.1), and let $h_i = x_i - x_{i-1}$. Using central differences for the x derivatives we may write (11) as,

$$\frac{(\psi_x)_{i+1/2,j}^2 - (\psi_x)_{i-1/2,j}^2}{h_i + h_{i+1}} + (\psi_{YY})_{i,j} = 0,$$

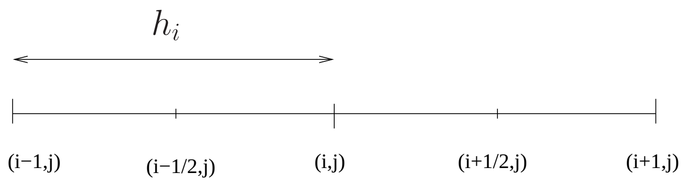

Fig. 1. Definition of the grid in the x direction

or,

$$\frac{1}{h_i + h_{i+1}}((\psi_x)_{i+1/2,j} - (\psi_x)_{i-1/2,j}).$$
$$.((\psi_x)_{i+1/2,j} + (\psi_x)_{i-1/2,j}) + (\psi_{YY})_{i,j} = 0. \tag{12}$$

As discussed in [1] if we have a subsonic point, the equation is elliptic and central differences should be used to calculate both $(\psi_x)_{i+1/2,j}$ and $(\psi_x)_{i-1/2,j}$. That is,

$$(\psi_x)_{i+1/2,j} = \frac{\psi_{i+1,j} - \psi_{i,j}}{h_{i+1}}$$
$$(\psi_x)_{i-1/2,j} = \frac{\psi_{i,j} - \psi_{i-1,j}}{h_i}.$$

If we write,

$$A_{i,j} = \frac{\psi_{i+1,j} - \psi_{i,j}}{h_{i+1}} - \frac{\psi_{i,j} - \psi_{i-1,j}}{h_i} \tag{13}$$

and, writing ψ_x in central differences as follows,

$$\psi_x^c = \frac{\psi_{i+1,j} - \psi_{i,j}}{h_{i+1}} + \frac{\psi_{i,j} - \psi_{i-1,j}}{h_i}$$

then we obtain, a new form of (13) as follows,

$$\frac{A_{i,j}}{h_i + h_{i+1}}\psi_x^c + (\psi_{YY})_{i,j} = 0. \tag{14}$$

If, we say that,

$$p_{i,j} = \frac{A_{i,j}}{h_i + h_{i+1}}\psi_x^c,$$

then, we may write (14) as,

$$p_{i,j} + (\psi_{YY})_{i,j} = 0. \tag{15}$$

If the point (i,j) is supersonic, then equation (12) becomes hyperbolic and backwards differences should be used to calculate both $(\psi_x)_{i+1/2,j}$ and $(\psi_x)_{i-1/2,j}$. That is,

$$(\psi_x)_{i+1/2,j} = \frac{\psi_{i,j} - \psi_{i-1,j}}{h_i}$$
$$(\psi_x)_{i-1/2,j} = \frac{\psi_{i-1,j} - \psi_{i-2,j}}{h_{i-1}}.$$

If, we say that,

$$A_{i-1,j} = \frac{\psi_{i,j} - \psi_{i-1,j}}{h_i} - \frac{\psi_{i-1,j} - \psi_{i-2,j}}{h_{i-1}}$$

and, writing ψ_x in backwards differences as follows,

$$\psi_x^b = \frac{\psi_{i,j} - \psi_{i-1,j}}{h_i} + \frac{\psi_{i-1,j} - \psi_{i-2,j}}{h_{i-1}},$$

$$p_{i-1,j} = \frac{A_{i-1,j}}{h_i + h_{i-1}}\psi_x^b$$

then, we may rewrite (12) as follows,

$$p_{i-1,j} + (\psi_{YY})_{i,j} = 0. \tag{16}$$

In order to jump from one finite difference scheme to another according to the type of point we have, [10] suggests the use of artificial viscosity $\mu_{(i,j)}$. Using the table below, instead of equations (16) and (15) we would have,

$$p_{i,j}(1 - \mu_{i,j}) + p_{i-1,j}\mu_{i-1,j} + \psi_{YY} = 0$$

TYPE OF POINT	ψ_x^c	ψ_x^b	$\mu_{i-1,j}$	$\mu_{i,j}$
ELLIPTIC	> 0	> 0	0	0
HYPERBOLIC	< 0	< 0	1	1
SONIC	< 0	> 0	0	1
SHOCK	> 0	< 0	1	0

TABLE I
TABLE 1. ARTIFICIAL VISCOSITY TABLE.

Note that a shock point can be seen as an addition of both elliptic and hyperbolic x difference operators. Another way to deal with a shock point is, (provided we have a weak shock (in which case vorticity can be neglected)) is to use the Murman shock point operator [1]. In our codes we treated a shock point using the Murman shock point operator.

In the Y direction, the physical domain was first truncated to y_∞ and mapped into the Chebyshev space, as in [Canuto, 1998] [12],

$$Y \in [0, y_\infty] \rightarrow z \in [-1, 1]$$

where,

$$z_j = \cos(\frac{j\pi}{N}), j = 0, 1, ..., N$$

and,

$$Y_j = y_\infty(\frac{z_j + 1}{2}).$$

In order to calculate first and second derivatives in the Y direction we use,

$$(\psi_Y)_{i,j} = \sum_{k=0}^{N} D_{1j,k}\psi_{i,k}$$

$$(\psi_{YY})_{i,j} = \sum_{k=0}^{N} D_{2j,k}\psi_{i,k}$$

where $D1_{j,k}$ and $D2_{j,k}$ represent the elements of the Chebyshev collocation differentiation matrices of first and second orders, as described in [12].

After applying the above discretizations we obtain a set of coupled nonlinear algebraic equations. These are linearized using Newton-Raphson linearization by setting

$$\psi_{i,j} = \overline{\psi_{i,j}} + G_{i,j},$$

where $\overline{\psi_{i,j}}$ represents the value of $\psi_{i,j}$ in a previous iteration and $G_{i,j}$ represents the update for $\psi_{i,j}$. This results in a linear system of equations for the $G_{i,j}$ of the form

$$\begin{aligned} A_{i,j}G_{i-2,j} + B_{i,j}G_{i-1,j} + C_{i,j}G_{i,j} \\ +H_{i,j}G_{i+1,j} + E_{i,j}G_{i+2,j} = F_{i,j} \end{aligned} \tag{17}$$

where, for example in the interior of the flow domain,

$$A_{i,j} = \frac{2\mu_{i-1,j}}{h_{i-1}(h_i + h_{i-1})}\frac{\overline{\psi_{i-1,j}} - \overline{\psi_{i-2,j}}}{h_{i-1}}$$

$$\begin{aligned} B_{i,j} = & \frac{2(1-\mu_{i,j})}{h_{i+1}(h_i + h_{i+1})}\frac{\overline{\psi_{i,j}} - \overline{\psi_{i-1,j}}}{h_i} + \\ & \frac{\mu_{i-1,j}}{(h_i + h_{i-1})}((\frac{-2}{h_i})\frac{\overline{\psi_{i,j}} - \overline{\psi_{i-1,j}}}{h_i} + \\ & \frac{\mu_{i-1,j}}{(h_i + h_{i-1})}(\frac{-2}{h_{i-1}})\frac{\overline{\psi_{i-1,j}} - \overline{\psi_{i-2,j}}}{h_{i-1}}) \end{aligned}$$

$$\begin{aligned} C_{i,j} = & \frac{(1-\mu_{i,j})}{(h_i + h_{i+1})}((\frac{-2}{h_{i+1}})\frac{\overline{\psi_{i+1,j}} - \overline{\psi_{i,j}}}{h_{i+1}} + \\ & +(\frac{-2}{h_i})\frac{\overline{\psi_{i,j}} - \overline{\psi_{i-1,j}}}{h_i}) + \\ & +\frac{2\mu_{i-1,j}}{h_i(h_i + h_{i-1})}\frac{\overline{\psi_{i,j}} - \overline{\psi_{i-1,j}}}{h_i} + D_2(i,j) \end{aligned}$$

$$H_{i,j} = \frac{1-\mu_{i,j}}{h_{i+1}(h_i + h_{i+1})}(\frac{2}{h_{i+1}})(\overline{\psi_{i,j}} - \overline{\psi_{i-1,j}});$$

$$E_{i,j} = 0$$

$$\begin{aligned} F_{i,j} = & -\frac{(1-\mu_{i,j})}{(h_i + h_{i+1})}(\frac{\overline{\psi_{i+1,j}} - \overline{\psi_{i,j}}}{h_{i+1}} - \\ & -\frac{\overline{\psi_{i,j}} - \overline{\psi_{i-1,j}}}{h_i})(\frac{\overline{\psi_{i+1,j}} - \overline{\psi_{i,j}}}{h_{i+1}} + \frac{\overline{\psi_{i,j}} - \overline{\psi_{i-1,j}}}{h_i}) \\ & -\beta_{i,j} - (\overline{\psi_{YY}})_{i,j} \end{aligned}$$

$$\begin{aligned} \beta_{i,j} = & \frac{\mu_{i-1,j}}{(h_i + h_{i-1})}(\frac{\overline{\psi_{i,j}} - \overline{\psi_{i-1,j}}}{h_i} - \frac{\overline{\psi_{i-1,j}} - \overline{\psi_{i-2,j}}}{h_{i-1}}). \\ & .(\frac{\overline{\psi_{i,j}} - \overline{\psi_{i-1,j}}}{h_i} + \frac{\overline{\psi_{i-1,j}} - \overline{\psi_{i-2,j}}}{h_{i-1}}). \end{aligned}$$

By writing $\mathbf{G_i} = (G_{i,0}, Gi, 1, \ldots, G_{i,N})^T$ the above equations can be written as

$$\mathbf{A_iG_{i-2} + B_iG_{i-1} + C_iG_i + H_iG_{i+1} + E_iG_{i+2} = F_i}$$

for $i = 1, \ldots, M$ where the $\mathbf{A_i}, \mathbf{B_i}, \mathbf{C_i}, \mathbf{H_i}, \mathbf{E_i}$, are $(N+1) \times (N+1)$ matrices, $\mathbf{F_i}$ is the $(N+1) \times 1$ vector of the right-hand side of (17) at the station $x = x_i$. Here M is the number of points in the x-direction. The block pentadiagonal system of equations was solved directly using the routines desscribed in [13]. Further details of the numerical method may be found in [14].

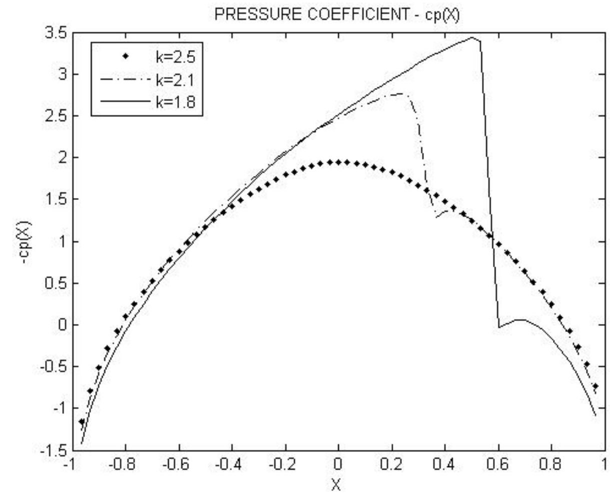

Fig. 2. Pressure coefficient C_p versus x for various values of the transonic similarity parameter k.

We consider an airfoil described by a parabolic arc $y = \delta(1-x^2)$ with x in $[-1, 1]$, where δ is the width of the airfoil. We have $\delta = 0.06$ and the angle of attack is zero. In fig. 2 we have shown the pressure coefficent for various values of the Mach number $M_\infty = 0.78, 0.82, 0.85$ corresponding to values of k the transonic similarity parameter being $k = 2.5, 2.1, 1.8$ respectively. For large values of k the flow is subsonic and free of shock. As k decreases a shock forms and moves closer to the trailing edge with increasing strength with k decreasing. The results shown in fig. 2 compare well with those in [10].

When testing the programme, we also considered other types of airfoil, namely the NACA0012 and all results were consistent with test cases present in literature such as [10], [17] and [18].

A. Some comments on grid size study.

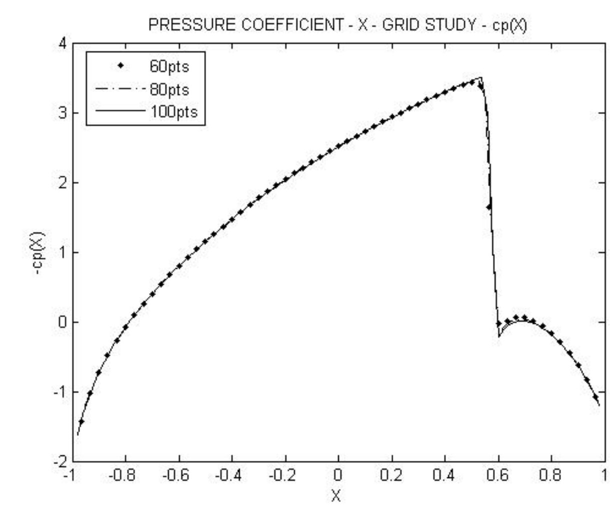

Fig. 3. Cp for $M_\infty = 0.85, \alpha = 0$ and for the parabolic circular arc aerofoil with ($M = 60, 80, 100$ points).

Various grid refinement studies have been carried to check for grid independence of the computed steady solutions. Generally the the solution is most sensitive to changes in the number of points in the x direction, but even then it is possible to obtain reasonable solutions with a relatively small number of points. In Fig. 3 we have shown the pressure coefficient for $k = 1.8$ taking varying number of points over the aerofoil.

A similar study was done for the number of Chebyshev points to consider in the Y direction and sample results can be seen in Fig. 4.

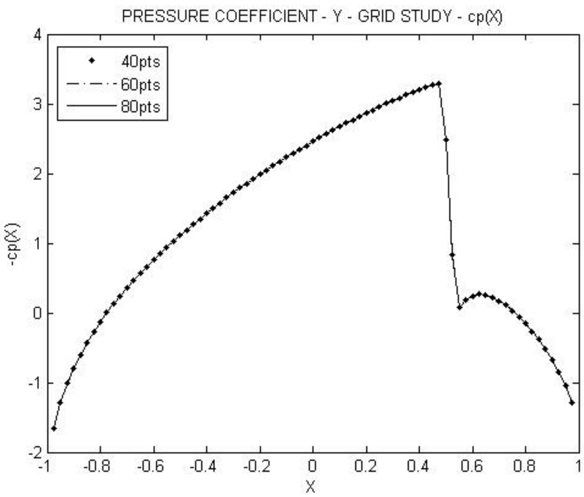

Fig. 4. Cp for $M_\infty = 0.85, \alpha = 0$ and for the parabolic circular arc aerofoil with ($N = 40, 60, 80$ points).

IV. The case for non symmetric airfoils

In the previous sections we presented a model that would solve the Kárman-Guderley equation for thin symmetric airfoils. Next we will show how to extend this code for non symmetric airfoils, including the Kutta condition. When we have a symmetric airfoil, we solve the Kárman Guderley equation just for one domain. When the airfoil is non symmetric, we have to solve the problem for the flow both above and below the aerofoil. The Kutta condition is used at the trailing edge to ensure that the jump obtained in the integration of ψ_x along the lower and upper surfaces at the tail is zero. This condition was introduced into the algorithm by:

Solve K-G equation for Upper domain

While not convergence

Solve K-G equation for Lower domain (with Kutta Condition).

Solve K-G equation for Upper domain (with Kutta Condition).

Verify convergence

End while

To start the algorithm results from the symmetric case were used as an initial guess.

V. Results for non symmetric case

The results we present next are for the test case of a NACA0012 airfoil at angle of attack=1.25°, and $M_\infty = 0.80$. The pressure coefficient is shown in Fig. 5 and agrees with the literature [1], [15], [16], amongst others.

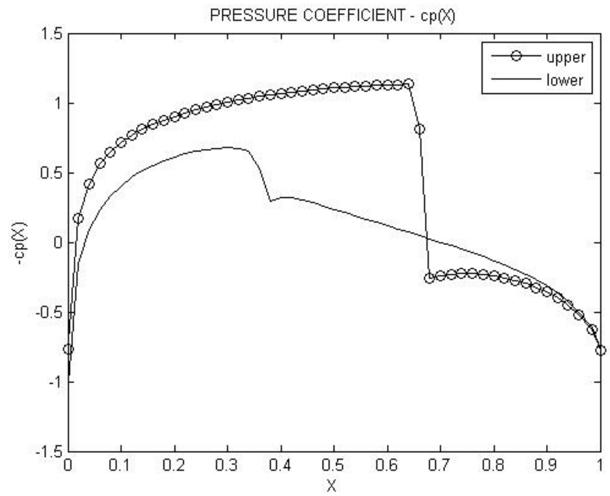

Fig. 5. Pressure coefficient for angle of attack=1.25°, $M_\infty = 0.80$ on the lower and upper surfaces.

In our case the lift coefficient was estimated to be $C_l = 0.3546$ which compares with the one by Oliveira (cited in [15]) $C_l = 0.3509$ and by Camilo $C_l = 0.3348$ [15]. In Fig. 6 we show results obtained for NACA0012 airfoil at angle of attack=2.0°, and $M_\infty = 0.80$.

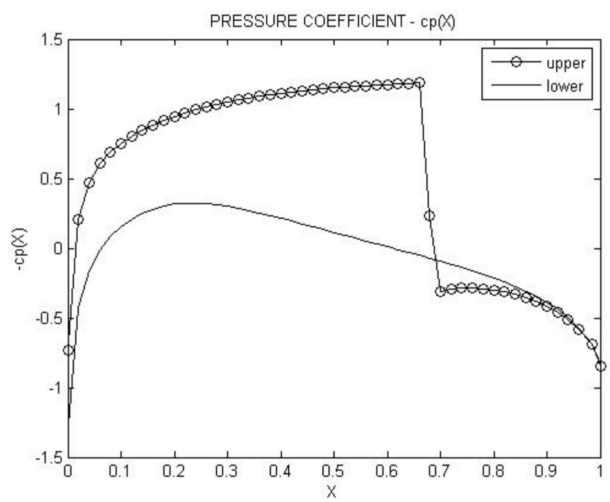

Fig. 6. Pressure coefficient for angle of attack=2.0°, $M_\infty = 0.80$ on the lower and upper surfaces.

VI. Considerations on stability of the flow for the non steady case

In order to discuss the stability of the flow one needs an unsteady version of the Kárman-Guderlay equation. Unsteady effects can be incorporated in many different ways, see for example [19], [20], but our starting point is the equation:

$$\phi_{xx}(k - \phi_x(\gamma + 1)) + \phi_{YY} = \beta\phi_{xt} \tag{18}$$

where,

$$\beta = 2\frac{M_\infty^2}{\delta^{\frac{2}{3}}}.$$

Note that (18) has the same left hand side as (4). Also the non-dimensional time variable t has been scaled to enable unsteady effects to appear at the same order as the nonlinearity in the Kárman-Guderlay equation. The unscaled non-dimensional time variable is $\delta^{-2/3}t$.

Using (8) we obtain,

$$\psi_x\psi_{xx} + \psi_{YY} = \beta\psi_{xt}. \tag{19}$$

If we consider that disturbances to an underlying base flow say $\psi_b(x, Y)$ are proportional to $e^{\lambda t}$, that is

$$\psi = \psi_b(x, Y) + \delta e^{\lambda t}\tilde{\psi}(x, y),$$

we obtain a partial differential eigenvalue problem for determining the eigenvalues λ and the eigenfunctions $\tilde{\psi}(x, y)$. After using the same discretization techniques described earlier the discrete equations can be assembled together in the form

$$[\mathbf{A}]\tilde{\psi} = \lambda[\mathbf{B}]\tilde{\psi} \tag{20}$$

which is a generalized eigenvalue problem. The flow is considered to be stable if the eigenvalue λ with the greatest real part is negative. In our case the coefficient matrix $\mathbf{A}$ in (20) is the same as the Jacobian matrix arising in the Newton linearisation of the base flow equations and of block pentadiagonal form. The matrix $\mathbf{B}$ is a singular matrix and in view of the ψ_{xt} term in (18), also not a diagonal matrix. The matrices are highly sparse square matrices of size $(N+1)^2M$ and even for modest sizes of N, M the solution of the eigenvalue problem can be challenging. The non-diagonal form of $\mathbf{B}$ means that it is not immediately possible (with the formulation as described above) to use the sparse matrix routines in MATLAB to calculate the eigenvalues. For small grids we used MATLAB with the inbuilt 'eigs', 'eig' and 'sptarn' routines, but these generate hundreds of eigenvalues and many of these are not physical. For example in Fig. 7 we show the eigenvalue spectrum for the case when $M_\infty = 0.8$, with 41 points over the wing and 45 Chebyshev points in the Y direction with zero angle of attack.

It can seen that there are many eigenvalues with very large imaginary parts. In the figure the eigenvalues with the greatest real part is $\lambda = 0.675 \pm 647i$, and this value changes significantly as the grid is refined suggesting that it is non-physical. The figure also shows many unstable eigenvalues and it is difficult to be able to discriminate between those which are physical or not without extensive grid size checks. For instance in Fig. 8 we show results with $M = 46$ and $N = 46$. The eigenvalues with the greatest real part are completely different now.

As the grid is refined the eigenvalue computations become computationally intensive with MATLAB both in terms of Cpu time as well as memory. For this reason we are currently investigating a different formulation of the unsteady problem in which it is possible to calculate only selected dominant eigenvalues and do grid refinement studies.

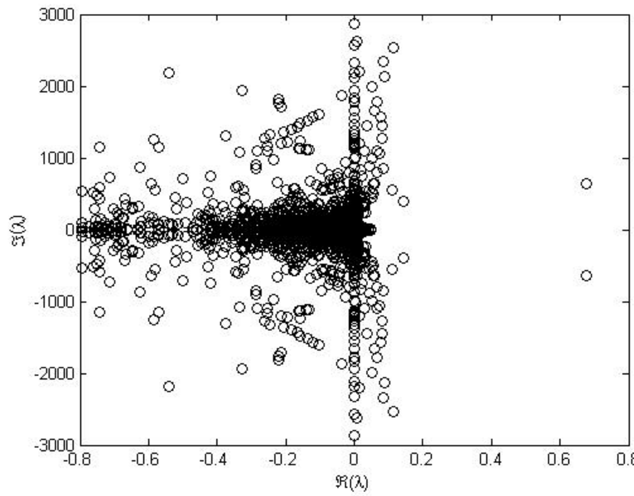

Fig. 7. Eigenvalue spectrum showing real and imaginary parts of λ for $M_\infty = 0.80, M = 41, N = 46$ for the NACA0012 aerofoil.

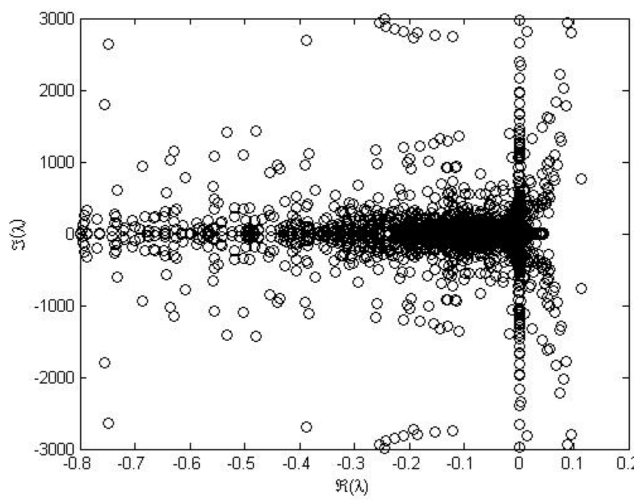

Fig. 8. Eigenvalue spectrum showing real and imaginary parts of λ for $M_\infty = 0.80, M = 46, N = 46$ for the NACA0012 aerofoil.

For example in Fig. 9, and Fig. 10 we have shown results for the unstable eigenvalues for the parabolic circular aerofoil for two cases $k = 2.3$ and $k = 1.8$ with much finer spatial resolutions. By varying N it is possible to obtain grid independent results but changes in M still generates quite different eigenvalues from grid to grid. Whilst it is not possible to make conclusive comments with regard to the physical and non-physical eigenvalues, it is clear that as the Mach number increases, the the flow 'stabilizes' with fewer unstable eigenvalues, and these have smaller growth rates, meaning that as the Mach number approaches 1 and the flow becomes supersonic instabilities in the flow tend to disappear. [Note also that in view of the scaling of the time variable, the actual growth rates are $O(\delta^{2/3}\lambda)$].

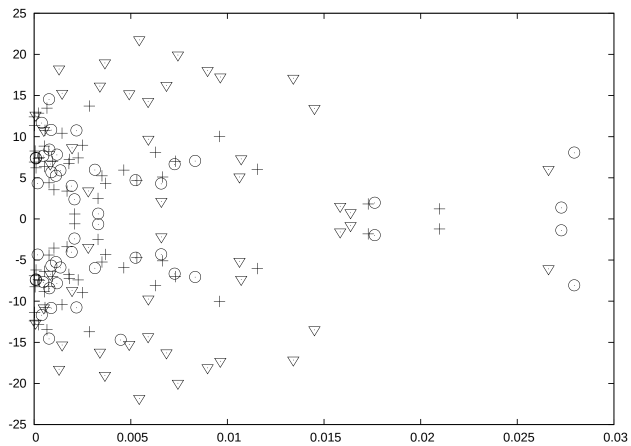

Fig. 9. Spectrum for $k = 2.3$ for circular arc aerofoil, + (M=300, N=70), ◯ (M=500, N=70), ▽ (M=100,N=47)

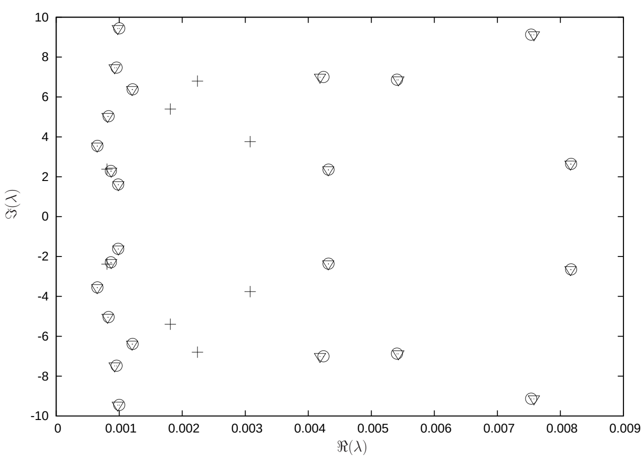

Fig. 10. Spectrum for $k = 1.8$ for circular arc aerofoil, + (M=200, N=47), ◯ (M=300, N=70), ▽ (M=300,N=90)

VII. Conclusions

- A new numerical method for calculating solutions to the Kárman-Guderlay equations for the flow past lifting and non-lifting aerofoils has been developed and found to work well.

- The method is particularly fast for symmetric aerofoils and requires just a few Newton iterations for convergence. With stronger shocks the number of iterations increases but with a good initial guess the method is still extremely robust.

- For the lifting case, as the Mach number increases or the angle of attack increases, the decoupling of the solution into computing the flow above and below the aerofoil works provided underrelaxation is used. A more direct approach would however be beneficial.

- The study that has been carried out to investigate the instability of the base flows computed was developed in MATLAB. Although MATLAB can be used to compute the eigenvalues, using the built in eigs, eig and sptarn functions, this is not particularly efficient either in terms of CPU time or memory. A different formulation of the problem looks more promising and will allow for systematic grid refinement studies.

- We have also developed new codes with the same approach programmed in Fortran so we can use much finer grids and do systematic grid refinement studies. Preliminary studies suggest that with the form of the unsteady equation used here, as the Mach number approaches 1, the global instability growth rates reduce significantly.

- It would be interesting to extend the hybrid method used here to the transonic small disturbance equation. Whereas for the Kárman-Guderlay equation the boundary conditions are applied on $Y = 0$, for the transonic small disturbance equation the boundary conditions need to be applied on the aerofoil surface. This makes the extension non-trivial.

Acknowledgements: The research was supported by the Centre of Mathematics (CMAT) of the University of Minho in Portugal.

References

[1] Cole, J. D. and Cook, L. P., *Transonic Aerodynamics*, Elsevier Science Publishers B.V., 1986.
[2] Caughey D., Jameson A., *Development of computational techniques for Transonic Flows; An historical perspective*,Symposium Transsonicum IV, Kluwer Academic, Gottingen, pp. 183-194, 2003.
[3] Holst, T. L., *Transonic flow computations using nonlinear potential methods*,Prog in Aero. Sci., 36, pp. 1-61, 2000.
[4] Jameson, A., *Transonic flow calculations*, Lecture Notes in Mathematics, Springer Verlag, 156-242, 1985.
[5] Tijdeman, H. and Seebass, R. , *Transonic flow past oscillating aerofoils*. Ann. Rev. Fluid. Mech., **12**, 181–222, 1980.
[6] Balakrishnan, A. V. , *Nonlinear Aeroelasticity: Continuum Theory, Flutter/Divergence Speed, and Plate Wing Model*, J. Aerospace Eng., **202**, pp. 194-202, 2006.
[7] Shubov, M. A., *Flutter Phenomenon in Aeroelasticity and Its Mathematical Analysis*, J. Aerospace Eng., **19**, pp. 1-12, 2006.
[8] V. B. L. Boppana and J. S. B. Gajjar, *Global flow instability in a lid-driven cavity*, Int. J. Num. Meth. in Fluids, (in press, but available online), 2009.
[9] R. P. Logue, J. S. B. Gajjar and A. I. Ruban, *Global stability of separated flows- subsonic flow past a corner*, Theo. Comp. Fluid Dyn., (submitted), 2010.
[10] Murman, E. M. and Cole, J. D.,*Calculation of plane steady transonic flows*. Boeing Scientific Research Laboratories, 1971.
[11] Murman, E. M. , *Analysis of embedded shock waves calculated by relaxation methods*. AIAA, Conf. Computational Fluid Dynamics, Palm Springs., 1973.
[12] Canuto, C., Hussaini, M. Y., Quarteroni, A., Zhang, T.A.,*Spectral Methods in Fluid Mechanics*. Springer series in Comp. Phys., Springer Verlag, 1998.
[13] Korolev G.L, Gajjar J.S.B., and Ruban A.I., *Once again on the supersonic flow separation near a corner* J. Fluid Mech., 463, 173-199, 2002.
[14] Pereira R. M. S., *Asymptotic theory of transonic viscous inviscid interaction*, Ph.D thesis, University of Manchester, 2005.
[15] Camilo E., *Soluo numrica das equaes de Euler para representao do escoamento transnico de aeroflios*. M.Sc thesis, University of São Paulo, Brazil,2003.
[16] Kudinov P.I., *Xoptimum - NACA 0012 transonic airfoil*, http://xoptimum.narod.ru/eng/results/ compressible/naca0012/naca0012.htm.
[17] Wang C. H. and Rusak Z., *Numerical studies on transonic BZT gas flows around thin airfoils* Journal of Fluid Dynamics, 1999, 396 pp 109-141, 1999.
[18] Hafez M. and Lovell D., *Transonic small disturbance calculations including entropy corrections*, Numerical and physical aspects of aerodynamic flows, T. Cabeci, Springer Verlag., 1981.

[19] Landahl, M. T., *Unsteady Transonic Flow*, Cambridge Univ. Press.,1989.
[20] Rizetta, D. P. and Chin, *Effect of frequency in unsteady transonic flow computations*, AIAA J., **18(8)**, pp. 1008-1010, W. C. 1979.

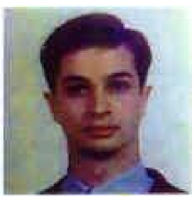

Rui M. S. Pereira is an Assistant Professor in the Department of Mathematics and Applications in The University of Minho in Portugal. PhD degree in Mathematical Sciences in the University of Manchester in 2005 in the United Kingdom. His current research interests are in areas of Transonic Flows, development of Indicators to measure the efficiency of water use in agriculture, mechanics and development of new e learning objects for students in Mathematics courses . He has published several research papers and appeared in journals such as Journal of Fluid Mechanics and proceedings of major conferences such as WSEAS , ASME ,World Water Congress, etc.

Jitesh S.B. Gajjar Jitesh Gajjar is Professor of Applied Mathematics in the School of Mathematics at the University of Manchester in the United Kingdom. He graduated with a Ph.D. degree in 1984 from Imperial College, London. His current interests are in the areas of theoretical and computational fluid dynamics specialising in flows at large Reynolds numbers, hydrodynamic stability theory, laminar separation. He has published extensively in leading journals, see http://www.maths.manchester.ac.uk/∼gajjar